Prethermalization and thermalization in entanglement dynamics

Bruno Bertini [1] and Pasquale Calabrese[2,3]

[1]*Department of Physics, Faculty of Mathematics and Physics, University of Ljubljana, Jadranska 19, SI-1000 Ljubljana, Slovenia*
[2]*SISSA and INFN, Sezione di Trieste, via Bonomea 265, I-34136, Trieste, Italy*
[3]*International Centre for Theoretical Physics (ICTP), I-34151, Trieste, Italy*

We investigate the crossover of the entanglement entropy toward its thermal value in nearly integrable systems. We employ equations-of-motion techniques to study the entanglement dynamics in a lattice model of weakly interacting spinless fermions after a quantum quench. For weak enough interactions we observe a two-step relaxation of the entanglement entropies of finite subsystems. Initially, the entropies follow a nearly integrable evolution, approaching the value predicted by the generalized Gibbs ensemble (GGE) of the unperturbed model. Then, they start a slow drift toward the thermal stationary value described by a standard Gibbs ensemble (GE). While the initial relaxation to the GGE is independent of the interaction, the slow drift from GGE to GE values happens on timescales proportional to the inverse interaction squared. For asymptotically large times and subsystem sizes the dynamics of the entropies can be predicted using a modified quasiparticle picture that keeps track of the evolution of the fermionic occupations caused by the integrability breaking. This picture gives a quantitative description of the results as long as the integrability-breaking timescale is much larger than the one associated with the (quasi)saturation to the GGE. In the opposite limit, the quasiparticle picture still provides the correct late-time behavior, but it underestimates the initial slope of the entanglement entropy.

The nonequilibrium dynamics of the entanglement in many-body systems is currently attracting huge attention, effectively bridging the gap between condensed matter, quantum information, and high-energy physics. Some of the big questions in this context concern the onset of thermalization in isolated many-body systems [1–4], the origin of thermodynamic entropy [5–11], the scrambling of quantum information in quantum chaotic systems [12–22], as well as the simulability of the quantum many-body dynamics via classical computers [23–27].

A fascinating aspect of this problem lies in its universality: the entanglement dynamics does not seem to depend much on the microscopic details of the many-body system. For instance, considering a quantum quench from a separable state one typically observes linear growth of the entanglement followed by saturation. When first observed in the context of $(1 + 1)$-dimensional conformal field theory (CFT), this phenomenon has been explained assuming that the entanglement is transported by pairs of correlated quasiparticles [28]. This intuitive *quasiparticle picture* can be used in systems with stable quasiparticle excitations, such as free [29–39] and interacting [40–45] integrable models, but it does not account for the fact that the same qualitative behavior is also observed in systems with no detectable quasiparticle content such as holographic CFTs [12,16,17] or generic interacting systems [46–55]; in essence, the only known cases where the entanglement does not behave as described above are connected with localization [56–62], quenched disorder [63,64], confinement [65–69], or presence of quantum scars [70,71].

Recently, an alternative explanation for the universality of the entanglement dynamics has arisen by studying the so-called (local) random unitary circuits [72], where the dynamics is completely random in space and the only constraint is given by the locality of interactions. In this case, one quantifies the amount of entanglement between two portions of the system by measuring the surface of the minimal space-time membrane separating them. This *minimal membrane picture* has been analytically tested in random unitary circuits [73] and it is believed to describe, at least qualitatively, the entanglement spreading in generic (nonintegrable) systems in any spatial dimension (see Ref. [74] for quantitative comparisons).

The two pictures discussed above rely on very different physical mechanisms and in general give different predictions. For instance, their predictions for the dynamics of the entanglement of disjoint regions [12,21] or that of a connected region in finite volume [22,51,72] are qualitatively different. In essence, while correlated quasiparticles produce disentanglement whenever the pairs find themselves in the same subsystem in the course of the evolution, no disentanglement is observed in the nonintegrable case. A natural question is then what happens to the entanglement dynamics when the integrability is broken only weakly. In this case, one would expect the two different mechanisms underlying the above picture to somehow coexist until the metastable quasiparticles decay.

Weakly nonintegrable systems are per se very interesting. Indeed, recent theoretical [75–100] and experimental [101–103] investigations pointed out that these systems display crossovers from integrable to nonintegrable dynamics

that are reminiscent of those described by the celebrated Kolmogorov-Arnold-Moser theory in few-particle classical integrable systems. The intuitive picture is that approximate conservation laws in the system generate a *separation of timescales* [96]. A symmetry-breaking term of order U becomes effective over a timescale that increases with $1/U$. For small enough U this is much larger than the relaxation time and the system relaxes as if the approximate conservation law were exact [80]. At later times, the symmetry breaking becomes effective and observables drift toward the true equilibrium state [88]. This phenomenon, dubbed *prethermalization* [75], is of crucial practical importance: it shows that integrability, although fragile, can be *dynamically robust* and hence *observable*. This is the ultimate explanation of why many cold-atom experiments detect traces of integrable many-body dynamics [104–107].

A major obstacle is that, aside from being physically very rich, the *prethermalization regime* is also very hard to access. One needs to follow the out-of-equilibrium dynamics of the (strictly speaking nonintegrable) system for very long times and the methods (both analytical and computational) to do that are very scarce. One might try to access this regime in some special class of nonintegrable systems, like the recently discovered dual-unitary quantum circuits [108], which led to the only available exact results on the entanglement dynamics in locally interacting nonintegrable systems [51,52,54]. However, even though these systems allow to study the weakly nonintegrable regime, the aforementioned results on the entanglement dynamics turn out to be independent of the integrability breaking. In this paper, we follow an alternative route and address this question focusing on what is arguably the simplest nontrivial setting. We consider a system of weakly interacting fermions on the lattice, which we analyze by means of equations-of-motion techniques [88,88,89,109–117]. This is an approximate method based on the truncation of the infinite hierarchy of evolution equations for connected fermionic cumulants of increasing size [equivalent to the Bogoliubov-Born-Green-Kirkwood-Yvon (BBGKY) hierarchy for reduced density operators [89,117]]. Our main finding is the identification of a regime, integrability breaking much smaller than inverse subsystem size, where the entanglement dynamics is quantitatively described for all times by a modified quasiparticle picture in which the contribution of each pair to the entanglement is (slowly) time dependent.

The rest of this paper is laid out as follows. In Sec. I we introduce the model and its basic properties. In Sec. II we describe the setting considered and briefly recall some basic facts about equations of motion. In Sec. III we discuss our results for the dynamics of the entanglement, and, in Sec. IV, we interpret them in terms of a modified quasiparticle picture. Finally, in Sec. V we report our conclusions.

I. MODEL

We consider a system of weakly interacting spinless fermions on a one-dimensional lattice of length L whose dynamics are described by the following Hamiltonian:

$$H[J_2, \delta, U] = H_1 + H_2 + H_U,$$

$$H_1 = -J_1 \sum_{l=1}^{L} [1 + (-1)^l \delta](c_l^\dagger c_{l+1} + \text{H.c.}),$$

$$H_2 = -J_2 \sum_{l=1}^{L} [c_l^\dagger c_{l+2} + \text{H.c.}],$$

$$H_U = U \sum_{l=1}^{L} n_l n_{l+1}. \tag{1}$$

Here $c_i^\dagger$ and c_i are, respectively, fermionic creation and annihilation operators obeying the canonical anticommutation relations

$$\{c_i^\dagger, c_j\} = \delta_{i,j}, \quad \{c_i, c_j\} = 0, \tag{2}$$

and we imposed periodic boundary conditions $c_{L+1} \equiv c_1$. For definiteness, from now on we consider the length L to be even and set $J_1 = 1$.

As discussed in Refs. [88,89] the Hamiltonian is integrable for $U = 0$, where it describes free fermions, and for $\delta = J_2 = 0$, where it can be mapped into a XXZ spin-$\frac{1}{2}$ chain in an external magnetic field [118] through a Jordan-Wigner transformation. Moreover for $J_2 = 0$ and $\delta, U \ll 1$ its low-energy description is given by the quantum sine-Gordon model [119]. Away from these points $H[J_2, \delta, U]$ is believed to be nonintegrable. This is confirmed the statistics of the level spacing of its unfolded spectrum. As shown in Fig. 1, level spacings are well described by the Gaussian orthogonal ensemble (GOE) of random matrices.

Since we are interested in the regime of small interactions, it is convenient to diagonalize the quadratic part of the Hamiltonian. This is achieved by the following linear mapping (see the Supplemental Material of Ref. [88])

$$c_l = \frac{1}{\sqrt{L}} \sum_{k>0} \sum_{\eta=\pm} \gamma_\eta(l, k|\delta) \alpha_\eta(k). \tag{3}$$

Here the sum runs over $k \in 2\pi/L \, \mathbb{Z}_{L/2} \subset [0, \pi]$ and

$$\gamma_\pm(2j - 1, k|\delta) = e^{-ik(2j-1)},$$

$$\gamma_\pm(2j, k|\delta) = \pm e^{-ik2j} e^{-i\varphi_k(\delta)},$$

$$e^{-i\varphi_k(\delta)} = \frac{-\cos k + i\delta \sin k}{\sqrt{\cos^2 k + \delta^2 \sin^2 k}}. \tag{4}$$

This transformation is a combination of a two-site discrete Fourier transform and a Bogoliubov transformation. In particular, it is immediate to see that it conserves the canonical anticommutation relations

$$\{\alpha_\mu(k), \alpha_\nu^\dagger(q)\} = \delta_{\mu,\nu} \delta_{k,q}. \tag{5}$$

Plugging (3) in (1) we find

$$H[J_2, \delta, U] = \sum_{\eta=\pm} \sum_{k>0} \epsilon_\eta(k) \alpha_\eta^\dagger(k) \alpha_\eta(k)$$
$$+ U \sum_{\boldsymbol{\eta}} \sum_{\boldsymbol{k}>0} V_{\boldsymbol{\eta}}(\boldsymbol{k}) \alpha_{\eta_1}^\dagger(k_1) \alpha_{\eta_2}^\dagger(k_2) \alpha_{\eta_3}(k_3) \alpha_{\eta_4}(k_4),$$
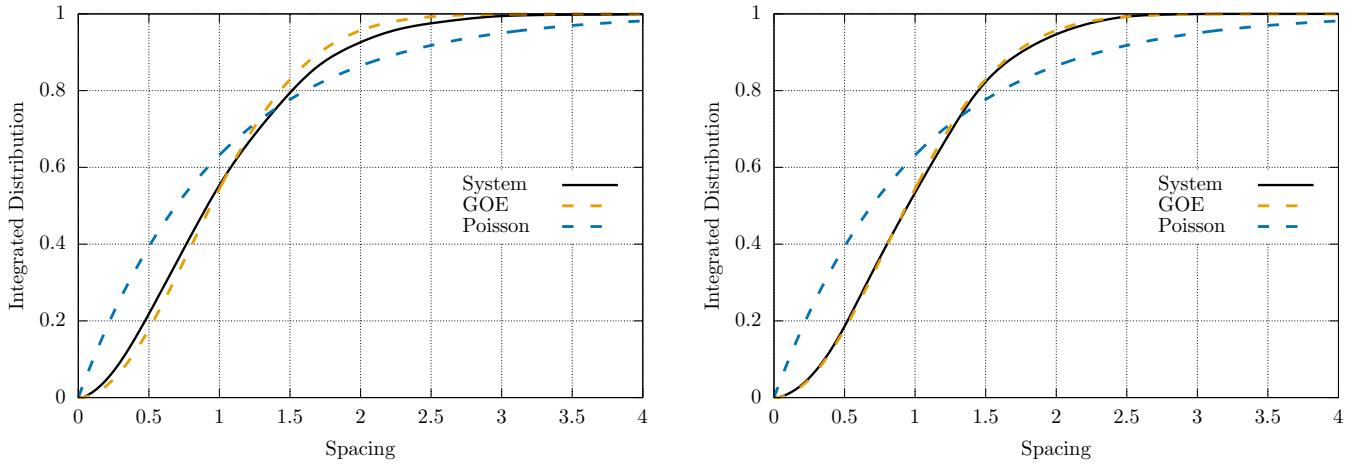
$$\tag{6}$$

FIG. 1. Cumulative (integrated) level-spacing distributions of (1) for $L = 16$ compared with Poisson and Wigner GOE distributions. Left panel: $\delta = 0.5$, $J_2 = 0$, $U = 1$. Right panel: $\delta = 0.5$, $J_2 = 0.5$, $U = 1$.

where bold symbols denote vectors with four components, namely, $\boldsymbol{\eta} = (\eta_1, \eta_2, \eta_3, \eta_4)$ and $\boldsymbol{k} = (k_1, k_2, k_3, k_4)$, we introduced the "dispersion relation"

$$\epsilon_\eta(k) = -2J_2 \cos(2k) + 2\eta\sqrt{\delta^2 + (1 - \delta^2)\cos^2(k)}, \quad (7)$$

and the "vertex function"

$$V_{\boldsymbol{\eta}}(\boldsymbol{k}) = -\frac{1}{4} \sum_{P,Q \in S_2} \text{sgn}(P)\text{sgn}(Q)$$

$$\times V'_{\eta_{p_1}\eta_{q_1}\eta_{p_2}\eta_{q_2}}(k_{p_1}, k_{q_1}, k_{p_2}, k_{q_2}). \quad (8)$$

Here we denoted by S_2 the group of permutations of two elements, we introduced

$$V'_{\boldsymbol{\eta}}(\boldsymbol{k}) \equiv \frac{e^{i(k_3 - k_4)}}{2L}[(M_{12} + M_{34})\delta_{k_1 - k_2 + k_3 - k_4, 0}$$

$$+ (M_{12} - M_{34})\delta_{k_1 - k_2 + k_3 - k_4 \pm \pi, 0}], \quad (9)$$

and finally

$$M_{ab} \equiv \left(\eta_a \eta_b e^{i\varphi_{k_a}(\delta) - i\varphi_{k_b}(\delta)}\right). \quad (10)$$

The physical interpretation of (6) is transparent. It describes two species of fermions ($+$ and $-$) interacting via two-body scattering.

II. SETTING

In this work we are interested in the dynamics of the entanglement generated by a quantum quench comparing the case where the evolution is free, $U = 0$, with that where it is weakly interacting, $0 < U \ll 1$. As it is customary, we characterize the entanglement evolution computing the entanglement entropies of a finite subsystem A in the thermodynamic limit. These are defined as

$$S_A^{(\alpha)}(t) \equiv \frac{1}{1 - \alpha} \log\left[\text{tr}\left[\rho_A^\alpha(t)\right]\right]. \quad (11)$$

Here $\rho_A(t)$ is the density matrix of the system at time t reduced to the subsystem A; α is known as Rényi index, it is an arbitrary positive real number, although in many circumstances it

is better to think of it as an integer. In the limit $\alpha \to 1$, the definition (11) is the standard von Neumann entropy of ρ_A.

Since we are interested in the dynamics of the entanglement *generated* by the quench, it is convenient to prepare the system in a low entangled initial state. To this aim, we consider the standard quantum quench protocol [120]: we prepare the system in the *ground state* $|\Psi_0\rangle$ of $H[J_{2i}, \delta_i, U_i]$ and, at $t = 0$, suddenly change the parameters

$$(J_{20}, \delta_0, U_0) \quad \longmapsto \quad (J_2, \delta, U). \quad (12)$$

After the quench the state of the system is then given by

$$|\Psi_t\rangle = e^{iH[J_2, \delta, U]t} |\Psi_0\rangle, \qquad t > 0. \quad (13)$$

In this work we will always focus on the case $U_0 = 0$ to ensure that Wick's theorem holds on the initial state (all connected cumulants with more than two fermionic operators vanish), as well as to have a well-defined GGE for the integrable quench [121]. These are mandatory requirements for the applicability of our techniques. Moreover, for definiteness, we also set $J_{20} = 0$.

Note that, due to the change in the dimerization parameter δ, the sudden quench (12) produces nontrivial dynamics also for vanishing interactions and it is meaningful to ask how this is influenced by U. Another possibility to observe the same scenario preserving translational invariance is to break the particle-number conservation in, e.g., the initial state. This, however, leads to a more complicated set of equations [89]. In this sense the Hamiltonian (1) represents the minimal model to study prethermalization in weakly interacting systems.

Using the mapping (3) we immediately find the following linear relations between the Bogoliubov fermions before ($\{\alpha_{0,\eta}^\dagger(k), \alpha_{0,\eta}(k)\}$) and after ($\{\alpha_\eta^\dagger(k), \alpha_\eta(k)\}$) the quench

$$\alpha_{0,\pm}(k) = \frac{1 \pm e^{i\Delta\varphi_k}}{2}\alpha_+(k) + \frac{1 \mp e^{i\Delta\varphi_k}}{2}\alpha_-(k), \quad (14)$$

where

$$\Delta\varphi_k \equiv \varphi_k(\delta_0) - \varphi_k(\delta). \quad (15)$$

A linear relation like (14) leads to a simple representation of the ground state of the prequench Hamiltonian in terms of the postquench Bogoliubov fermions (see, e.g.,

Refs. [120,122–124]). Specifically, in our case we find

$$|\Psi_0\rangle = \prod_{k>0}\left[\cos\left(\frac{\Delta\varphi_k}{2}\right)\alpha_-^\dagger(k) + i\,\sin\left(\frac{\Delta\varphi_k}{2}\right)\alpha_+^\dagger(k)\right]|0\rangle,$$

(16)

and $|0\rangle$ is the vacuum of the postquench Bogoliubov fermions $\{\alpha_\pm^\dagger(k),\alpha_\pm(k)\}$.

A. Free quench

For $U = 0$ the system is completely characterized by the occupation numbers, i.e., the expectation values of the (number-conserving) fermion bilinears on the time-evolving state (13):

$$n_{\mu\nu}(k,t) \equiv \langle\Psi_t|\alpha_\mu^\dagger(k)\alpha_\nu(k)|\Psi_t\rangle, \quad \mu,\nu = \pm.$$ (17)

Since the Hamiltonian (6) is quadratic we immediately have

$$n_{\mu\nu}(k,t) = n_{\mu\nu}(k)e^{i[\epsilon_\mu(k)-\epsilon_\nu(k)]t}.$$ (18)

Moreover, using the form (16) of the initial state we find

$$n_{\pm\pm}(k) = \frac{(1\mp\cos\Delta\varphi_k)}{2},$$

$$n_{\pm\mp}(k) = \frac{\mp i\,\sin(\Delta\varphi_k)}{2}.$$ (19)

We see that the diagonal occupation numbers are conserved (independent of time) while the off-diagonal are oscillating. This means that the expectation values of local (in space) observables for large times, and hence the generalized Gibbs ensemble, are completely specified only by the former; the contribution of the latter vanishes in a power-law fashion [120].

B. Weakly nonintegrable quench: Equations of motion

Whenever $U \neq 0$ the situation drastically complicates. Even though the occupation numbers completely characterize the system at $t = 0$ (because of the initial state we chose), as soon as the time evolution begins, nontrivial correlations start to build up resulting in nonzero higher connected cumulants. This means that

$$\langle\Psi_t|\alpha_{\mu_1}^\dagger(k_1)\dots\alpha_{\mu_n}^\dagger(k_n)\alpha_{\nu_1}(p_1)\dots\alpha_{\nu_n}(p_n)|\Psi_t\rangle$$ (20)

cannot be expressed in terms of (17) anymore. Equivalently, this means that the time-evolving state ceases to be Gaussian. Moreover, $n_{\mu\nu}(k,t)$ is no longer given by the simple expression (18): the evolution of the occupation numbers becomes nontrivially coupled to that of the higher cumulants.

Here we shall assume that, when a Gaussian state is evolving according to an interacting Hamiltonian with $U \ll 1$, there exists a (parametrically large) time window over which higher cumulants *remain small*. This leads to two key simplifications: (i) the state remains approximately Gaussian and we continue to characterize it by means of (17), (ii) the time evolution of the occupation numbers can be (approximately) determined. This assumption has been tested in Refs. [80,88,89] comparing the results for two- and four-point functions obtained in this way with time-dependent density-matrix renormalization group (tDMRG) simulations and exact diagonalization. Here, we will further test it in the case of the entanglement entropy, proving its consistency with exact diagonalization (ED) results.

To calculate the time evolution of (17) we use the equations of motion (EOM) [88,88,89,109–116]. These are a set of evolution equations for $n_{\mu\nu}(k,t)$ obtained by truncating the infinite hierarchy of evolution equations of the connected cumulants. We refer to the literature (see, e.g., Refs. [89,112,115,116]) for a detailed explanation of the method and only list the final equations. Specifically, we will follow the notation/conventions of Refs. [88,89] and consider two different truncation schemes respectively known as *first order* and *second order*. Their names are motivated by the fact that, at fixed t and small U, these two schemes give results that are accurate, respectively, to the first and second order in U. This, however, does not mean that these two schemes are equivalent to a first- or second-order perturbative expansion. On the contrary, they correspond to the resummation of a certain class of terms (infinitely many) in the perturbative series.

1. First-order EOM

The first-order truncation scheme leads to the following equations [89]:

$$\partial_t n_{\mu\nu}(k,t) = i\epsilon_{\mu\nu}(k)n_{\mu\nu}(k,t)$$
$$+ 4iU\sum_{\{\gamma_i\}}\sum_{q>0}\left[V_{\gamma_1\gamma_2\gamma_3\mu}(k,q,q,k)n_{\gamma_1\nu}(k,t)\right.$$
$$\left. - V_{\nu\gamma_2\gamma_3\gamma_1}(k,q,q,k)n_{\mu\gamma_1}(k,t)\right]n_{\gamma_2\gamma_3}(q,t).$$ (21)

As shown in Refs. [89,125] the results of these equations are equivalent to those found in Ref. [80] using the continuous unitary transformation (CUT) approach [75,126–129]. In essence, these equations describe the approach to the prethermal regime and the relaxation to the nonthermal deformed GGE of Ref. [80]. More specifically, for $t \gg 1$ one can expand the solution of (21) as follows [125]:

$$n_{\mu\nu}(k,t) = n_{\mu\nu}(k)e^{i[\epsilon_\mu^{dr}(k)-\epsilon_\nu^{dr}(k)]t} + Un_{\mu\nu}^{(1)}(k,t)e^{i[\epsilon_\mu^{dr}(k)-\epsilon_\nu^{dr}(k)]t} + O(U^2),$$ (22)

where

$$\epsilon_\eta^{dr}(k) = \epsilon_\eta(k) + 4U\sum_\gamma\sum_{q>0}V_{\eta\gamma\gamma\eta}(k,q,q,k)n_{\gamma\gamma}(q) + O(U^2),$$ (23)

$$n_{\mu\nu}^{(1)}(k,t) = 4\sum_{\{\gamma_i\}}\sum_{q>0}W_{\gamma_1\gamma_2\gamma_3\mu}(k,q)n_{\gamma_1\nu}(k)n_{\gamma_2\gamma_3}(q)\left[e^{i[\epsilon_{\gamma_1}^{dr}(k)+\epsilon_{\gamma_2}^{dr}(q)-\epsilon_{\gamma_3}^{dr}(q)-\epsilon_\mu^{dr}(k)]t} - 1\right]$$
$$- 4\sum_{\{\gamma_i\}}\sum_{q>0}W_{\nu\gamma_2\gamma_3\gamma_1}(k,q)n_{\mu\gamma_1}(k)n_{\gamma_2\gamma_3}(q)\left[e^{i[\epsilon_\nu^{dr}(k)+\epsilon_{\gamma_2}^{dr}(q)-\epsilon_{\gamma_3}^{dr}(q)-\epsilon_{\gamma_1}^{dr}(k)]t} - 1\right],$$ (24)

$$W_{\gamma_1\gamma_2\gamma_3\gamma_4}(k_1, k_2) = \lim_{B\to\infty} V_{\gamma_1\gamma_2\gamma_3\gamma_4}(k_1, k_2, k_2, k_1) \frac{1 - e^{-B|\epsilon_{\gamma_1}^{\rm dr}(k_1)+\epsilon_{\gamma_2}^{\rm dr}(k_2)-\epsilon_{\gamma_3}^{\rm dr}(k_2)-\epsilon_{\gamma_4}^{\rm dr}(k_1)|}}{\epsilon_{\gamma_1}^{\rm dr}(k_1) + \epsilon_{\gamma_2}^{\rm dr}(k_2) - \epsilon_{\gamma_3}^{\rm dr}(k_2) - \epsilon_{\gamma_4}^{\rm dr}(k_1)}, \tag{25}$$

and where also the higher orders in U do not contain secular terms. This expansion can be obtained, e.g., by a perturbative solution of (21) using the method of multiple scales of Ref. [130].

Before moving to the second-order scheme we make two final remarks. First, Eq. (21) [and hence the solution (22)] does not depend on J_2. Second, the solution (22) gives the following occupation numbers for the deformed GGE:

$$n_{\mu\nu}^{\rm dGGE}(k) = \begin{cases} n_{\mu\mu}(k) + 4U \sum_{\gamma_1\gamma_2} \sum_{q>0} \left[W_{\mu\gamma_1\gamma_2\bar\mu}(k, q)n_{\mu\bar\mu}(k) - W_{\bar\mu\gamma_1\gamma_2\mu}(k, q)n_{\mu\mu}(k) \right] n_{\gamma_1\gamma_2}(q), & \mu = \nu \\ 8U \sum_{\gamma} \sum_{q>0} W_{\mu\gamma\gamma\bar\mu}(k, q)n_{\mu\bar\mu}(k)n_{\gamma\gamma}(q), & \mu = \bar\nu \end{cases} \tag{26}$$

where $\bar\mu = -\mu$.

2. Second-order EOM

The second-order truncation scheme (also known as second Born approximation [117]) leads to the following equations [89]:

$$\partial_t n_{\mu\nu}(k, t) = i\epsilon_{\mu\nu}(k)n_{\mu\nu}(k, t) + 4iU \sum_{\{\gamma_i\}} \sum_{q>0} V_{\gamma_1\gamma_2\gamma_3\mu}(k, q, q, k)e^{i\epsilon_{\gamma_1\nu}(k)t}e^{i\epsilon_{\gamma_2\gamma_3}(q)t}n_{\gamma_1\nu}(k)n_{\gamma_2\gamma_3}(q)$$
$$- 4iU \sum_{\{\gamma_i\}} \sum_{q>0} V_{\nu\gamma_2\gamma_3\gamma_1}(k, q, q, k)e^{i\epsilon_{\mu\gamma_1}(k)t}e^{i\epsilon_{\gamma_2\gamma_3}(q)t}n_{\mu\gamma_1}(k)n_{\gamma_2\gamma_3}(q)$$
$$- U^2 \int_0^t dt' \sum_{\bar\gamma} \sum_{k_1,k_2,k_3>0} L_{\mu\nu}^{\bar\gamma}(k_1, k_2, k_3; k; t - t')n_{\gamma_1\gamma_2}(k_1, t')n_{\gamma_3\gamma_4}(k_2, t')n_{\gamma_5\gamma_6}(k_3, t')$$
$$- U^2 \int_0^t dt' \sum_{\gamma} \sum_{k_1,k_2>0} K_{\mu\nu}^{\gamma}(k_1, k_2; k; t - t')n_{\gamma_1\gamma_2}(k_1, t')n_{\gamma_3\gamma_4}(k_2, t'), \tag{27}$$

where we denoted vectors of length six by $\bar\gamma$, while the kernels are given by

$$K_{\mu\nu}^{\gamma}(k_1, k_2; k; t) \equiv 4 \sum_{k_3,k_4>0} \sum_{\eta,\eta'} X_{\bm{k};\bm{k}'}^{\gamma_1\gamma_3\eta\eta';\eta\eta'\gamma_4\gamma_2}(\mu, \nu; k; t), \tag{28}$$

$$L_{\mu\nu}^{\bar\gamma}(k_1, k_2, k_3; k; t) \equiv 8 \sum_{\eta} \sum_{k_4>0} X_{\bm{k};\bm{k}'}^{\gamma_1\gamma_3\gamma_6\eta;\eta\gamma_5\gamma_4\gamma_2}(\mu, \nu; k; t) - 16 \sum_{\eta} X_{k_1k_2k_1k_2;k_3k_1k_3k_1}^{\gamma_1\gamma_3\eta\gamma_4;\gamma_5\eta\gamma_6\gamma_2}(\mu, \nu; k; t). \tag{29}$$

Here, $\bm{k}'$ is obtained from $\bm{k}$ by reversing the order of the elements and we introduced

$$X_{\bm{k};\bm{q}}^{\gamma;\eta}(\mu, \nu; q; t) \equiv Y_{\mu\nu}^{\gamma}(\bm{k}, \bm{q})V_{\eta}(\bm{q})e^{iE_{\gamma}(k)t} - (\gamma, \bm{k}) \leftrightarrow (\eta, \bm{q}), \tag{30}$$

$$E_{\eta}(\bm{q}) \equiv \epsilon_{\eta_1}(q_1) + \epsilon_{\eta_2}(q_2) - \epsilon_{\eta_3}(q_3) - \epsilon_{\eta_4}(q_4), \tag{31}$$

$$Y_{\mu\nu}^{\eta}(k, \bm{q}) \equiv \delta_{\nu,\eta_4}\delta_{k,q_4}V_{\eta_1\eta_2\eta_3\mu}(\bm{q}) + \delta_{\nu,\eta_3}\delta_{k,q_3}V_{\eta_1\eta_2\mu\eta_4}(\bm{q})$$
$$- \delta_{\mu,\eta_2}\delta_{k,q_2}V_{\eta_1\nu\eta_3\eta_4}(\bm{q}) - \delta_{\mu,\eta_1}\delta_{k,q_1}V_{\nu\eta_2\eta_3\eta_4}(\bm{q}). \tag{32}$$

As shown in Refs. [88,89], for $0 \leqslant t \lesssim U^{-1}$ the two-point functions computed with (27) remain order U close to those

computed with (21), providing a perturbative correction. For $t \gg U^{-1}$, however, the solutions of (27) leave the prethermal plateau describing a drift of two-point functions toward their thermal value [88,89], although the EOM method is not guaranteed to capture all features emerging at asymptotically large times [131,132].

In the late-time regime the time integrals in (27) can be simplified [89] obtaining a local-in-time quantum Boltzmann equation (QBE) [112–115] (see also [97–99] for recent generalizations of the QBE to treat interacting integrable systems). More precisely, considering the scaling limit

$$U \to 0 \quad \text{and} \quad t \to \infty \quad \text{with} \quad \tau = tU^2 \quad \text{fixed,} \tag{33}$$

and filtering out highly oscillating terms (which do not contribute to local observables) one obtains the following equation for the diagonal occupation numbers [89]:

$$\partial_\tau n_{\mu\mu}(k, \tau) = - \sum_{\eta,\gamma} \sum_{p,q>0} \widetilde{K}_{\mu}^{\gamma\eta}(p, q|k)n_{\gamma\gamma}(p, \tau)n_{\eta\eta}(q, \tau) - \sum_{\gamma,\eta,\varphi} \sum_{p,q,r>0} \widetilde{L}_{\mu}^{\gamma\eta\varphi}(p, q, r|k)n_{\gamma\gamma}(p, \tau)n_{\eta\eta}(q, \tau)n_{\varphi\varphi}(r, \tau). \tag{34}$$

Here the kernels are given by

$$\widetilde{K}_\alpha^{\gamma_1\gamma_2}(k_1, k_2|q) \equiv 4 \sum_{k_3,k_4>0} \sum_{\nu,\nu'} \widetilde{X}_{\bm{k}|\bm{k}'}^{\gamma_1\gamma_2\nu\nu'|\nu\nu'\gamma_2\gamma_1}(\alpha|q),$$

$$\widetilde{L}_\alpha^{\gamma_1\gamma_2\gamma_3}(k_1, k_2, k_3|q) \equiv 8 \sum_{\nu} \sum_{k_4>0} \widetilde{X}_{\bm{k}|\bm{k}'}^{\gamma_1\gamma_2\gamma_3\nu|\nu\gamma_3\gamma_2\gamma_1}(\alpha|q) - 16 \sum_{\nu} \widetilde{X}_{k_1k_2k_1k_2|k_3k_1k_3k_1}^{\gamma_1\gamma_2\nu\gamma_2|\gamma_3\nu\gamma_3\gamma_1}(\alpha|q),$$

$$\widetilde{X}_{\bm{k}|\bm{q}}^{\gamma|\alpha}(\alpha|q) \equiv Y_{\alpha\alpha}^\gamma(\bm{k}, q)V_\alpha(\bm{q})D(E_\gamma(\bm{k})) - (\bm{\gamma}, \bm{k}) \leftrightarrow (\bm{\alpha}, \bm{q}),$$

$$D(E) \equiv \lim_{\xi \to 0} \frac{i}{E + i\xi}. \tag{35}$$

As initial value for the quantum Boltzmann equation one takes the diagonal occupation numbers $\{n_{\pm\pm}(k, t_0)\}$ produced by the second-order EOM (27) for large enough t_0 (corresponding to the deformed GGE values).

It can be verified (see, e.g., [89,115]) that noninteracting Fermi-Dirac distribution (with arbitrary β and μ) is always a stationary solution of the QBE. Moreover, for nonintegrable models the latter is believed to be the only stationary solution [115]. The specific values of temperature and chemical potential can be determined from the initial conditions by noting that the QBE conserves number density and the kinetic energy. This means that in our case we expect the QBE to describe relaxation to a "free Gibbs ensemble," reproducing the solution of the second-order EOM (27) only up to $O(U)$ corrections. Importantly, this is enough to observe the transition between GGE and thermal values because their difference is $O(U^0)$, i.e., they are different even for $U = 0$.

III. ENTANGLEMENT ENTROPY FROM EOM

We compute the entropies under the assumption that the state remains approximately Gaussian for $t > 0$. This assumption is in principle stronger than the one used to derive (27). Indeed, in the derivation of (27) four-particle cumulant is approximated by a nonzero value [89]. We expect that, however, in the time window of validity of the EOM this approximation gives the leading order (in U) of the entropies.

Under the Gaussian-state assumption we can directly compute the entanglement entropy from the correlation matrix

$$\begin{aligned} C_{ij}(t) &= \langle\Psi_t|c_i^\dagger c_j|\Psi_t\rangle \\ &= \frac{1}{L}\sum_{k>0}\sum_{\mu,\nu=\pm}\gamma_\mu^*(k, i)\gamma_\nu(k, j)n_{\mu\nu}(k, t) \end{aligned} \tag{36}$$

as follows [133–135]:

$$S_A^{(\alpha)}(t) \equiv \frac{1}{1-\alpha}\mathrm{tr}\log[C^\alpha + (1-C)^\alpha]. \tag{37}$$

Note that this form is particularly simple because the correlations $\langle\Psi_t|c_i^\dagger c_j^\dagger|\Psi_t\rangle$ and $\langle\Psi_t|c_i c_j|\Psi_t\rangle$ are zero at all times. This is a consequence of both the initial state and the Hamiltonian being U(1) invariant (the initial state has a fixed number of fermions and the Hamiltonian conserves it).

To test the EOM predictions, we compute the entropy of the thermal state using exact diagonalization (ED). More precisely, we evaluate numerically

$$S_{\mathrm{th}}^{(\alpha)} = \frac{1}{1-\alpha}\log\mathrm{tr}[\rho_{\mathrm{th}}^\alpha] \tag{38}$$

in two different ways to estimate the finite-size corrections. First, we used the canonical representation for the thermal density matrix

$$\rho_{\mathrm{th}} = \frac{e^{-\beta H[J_2,\delta,U]}}{\mathrm{tr}[e^{-\beta H[J_2,\delta,U]}]}, \tag{39}$$

where the temperature is fixed by requiring

$$\mathrm{tr}[\rho_{\mathrm{th}}H[J_2, \delta, U]] = \langle\Psi_0|H[J_2, \delta, U]|\Psi_0\rangle. \tag{40}$$

In this representation the trace in (38) must be reduced to states with fixed particle number, namely, to a basis of the eigenspace of

$$N = \sum_{l=1}^L c_l^\dagger c_l, \tag{41}$$

corresponding to the eigenvalue $L/2$. Next, we consider the grand-canonical representation of ρ_{th}, namely,

$$\rho_{\mathrm{th}} = \frac{e^{-\beta(H[J_2,\delta,U]-\mu N)}}{\mathrm{tr}[e^{-\beta(H[J_2,\delta,U]-\mu N)}]}, \tag{42}$$

where temperature and chemical potential are fixed by requiring

$$\begin{aligned} \mathrm{tr}[\rho_{\mathrm{th}}H[J_2, \delta, U]] &= \langle\Psi_0|H[J_2, \delta, U]|\Psi_0\rangle, \\ \mathrm{tr}[\rho_{\mathrm{th}}N] &= \langle\Psi_0|N|\Psi_0\rangle = L/2. \end{aligned} \tag{43}$$

Finally, we extrapolate the results for $L \to \infty$ assuming

$$S_{\mathrm{th}}^{(\alpha)}(L) = S_{\mathrm{th}}^{(\alpha)}(\infty) + \frac{A^{(\alpha)}}{L} + O\left(\frac{1}{L^2}\right), \tag{44}$$

where $A^{(\alpha)}$ is a constant determined through a linear fit. This procedure is sometimes plagued by even-odd effects in the ED data, limiting its range of applicability.

Some representative examples of our results are reported in Figs. 2–4. We see that, while the first-order EOM (21) predict relaxation to a deformed GGE, the solution of the second-order EOM (27) shows a slow drift toward the thermal value computed by ED. Such a drift occurs on timescales $t \sim U^{-2}$ and is well described by the QBE (34), in agreement with the findings of Refs. [88,89]. In particular, this implies
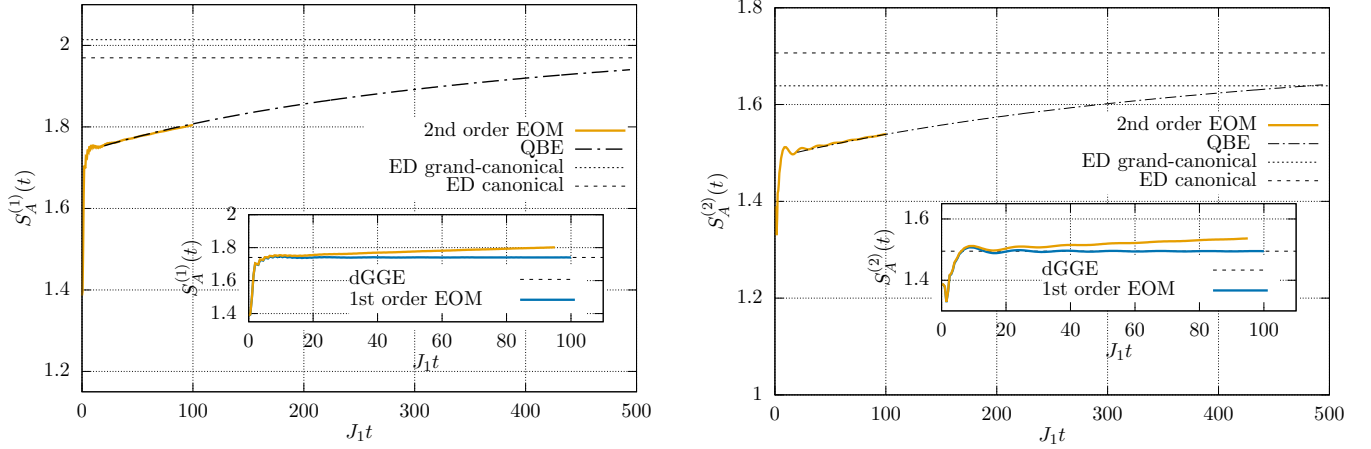
FIG. 2. Time evolution of the von Neumann entropy (left) and Renyi-2 entropy (right) after the quench (12) with parameters $J_{20} = 0$, $\delta_0 = 0.8$, $U_0 = 0$, $J_2 = 0.65$, $\delta = 0.1$, $U = 0.1$, and $|A| = 4$. Different lines report the predictions of the different methods and the insets present the late-time behavior computed via quantum Boltzmann equation (initialized at time $t_0 = 20.1$). The difference between canonical and grand-canonical prediction gives an estimation of the error in the extrapolation of the ED results.
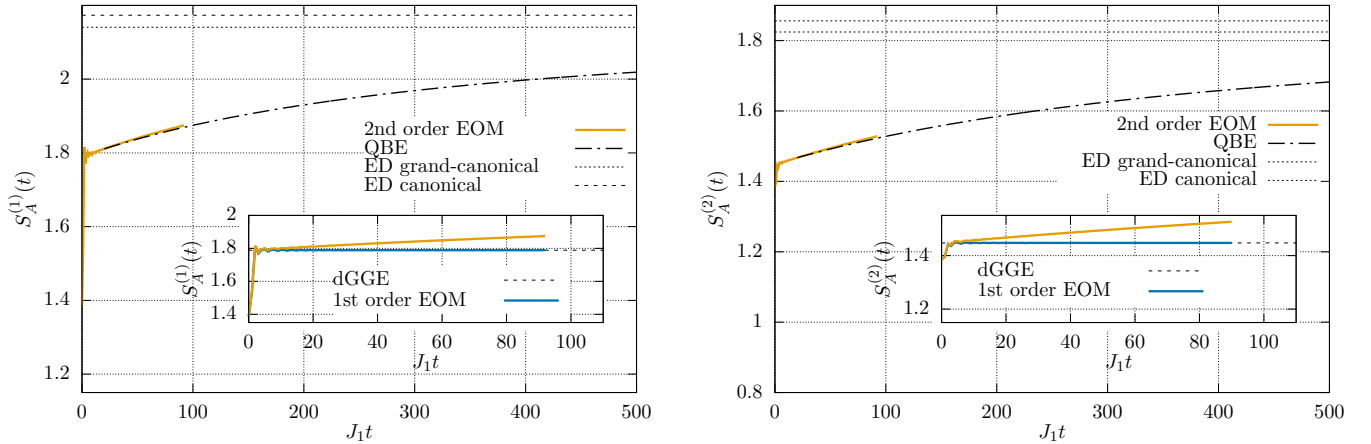

FIG. 3. Time evolution of the von Neumann entropy (left) and Renyi-2 entropy (right) after the quench (12) with parameters $J_{20} = 0$, $\delta_0 = 0.8$, $U_0 = 0$, $J_2 = 0.65$, $\delta = 0$, $U = 0.1$, and $|A| = 4$. Different lines report the predictions of the different methods and the insets present the late-time behavior computed via quantum Boltzmann equation (initialized at time $t_0 = 20.1$). The difference between canonical and grand-canonical prediction gives an estimation of the error in the extrapolation of the ED results.
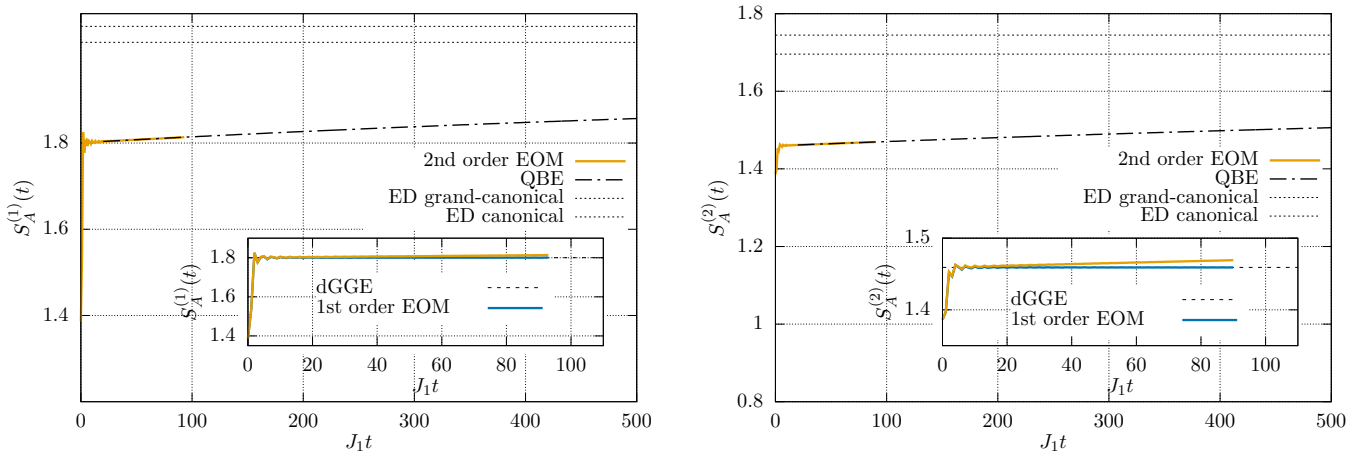

FIG. 4. Time evolution of the von Neumann entropy (left) and Renyi-2 entropy (right) after the quench (12) with parameters $J_{20} = 0$, $\delta_0 = 0.8$, $U_0 = 0$, $J_2 = 0.5$, $\delta = 0$, $U = 0.05$, and $|A| = 4$. Different lines report the predictions of the different methods and the insets present the late-time behavior computed via quantum Boltzmann equation (initialized at time $t_0 = 20.1$). The difference between canonical and grand-canonical prediction gives an estimation of the error in the extrapolation of the ED results.

that for large enough times the drift can be described by an exponential (as it is customary the characteristic time can be obtained by linearizing the QBE [109]).

Finally, we see that the speed of the drift is highly influenced by the value of the next-neighbor hopping term J_2. This has been explained in [88,89] (see also Refs. [115,136]) by noting that J_2 opens more *scattering channels* for the quasiparticles. To understand this point it is convenient to look at the Boltzmann equation (34). We see that the only scattering processes contributing to the right-hand side of this equation are those conserving energy and momentum (modulo π): the energy conservation is enforced by $D(E)$ while the momentum conservation by the vertex $V_{\boldsymbol{\alpha}}(\boldsymbol{q})$. A nonzero J_2 allows for more inelastic solutions of these constraints, namely, for processes

$$
t \uparrow \qquad
\begin{array}{cc}
(\alpha_f, k_f) & (\beta_f, p_f) \\
& \\
& \\
(\alpha_i, k_i) & (\beta_i, p_i)
\end{array}
\qquad , \qquad (45)
$$

with $\{(\alpha_i, k_i), (\beta_i, p_i)\} \neq \{(\alpha_f, k_f), (\beta_f, p_f)\}$. These are the scattering processes able to modify the momentum distribution.

IV. EOM AND QUASIPARTICLE PICTURE

In the integrable case the initial state (16) can be viewed as a source of $+$ and $-$ quasiparticles, where those with the same momentum k are correlated. This can be understood by noting that the eigenstates of $H[J_2, \delta, 0]$ with nonzero overlap with $|\Psi_0\rangle$ feature only one of the modes $(+, k)$ and $(-, k)$, such a nontrivial microscopic constraint generates the correlation [37]. For $t, |A| \gg 1$ we can then describe the evolution of the entanglement entropies at the leading order using the quasiparticle picture [28,40]. Writing the prediction in the case of correlated pairs with different velocities we have

$$
S_{\mathrm{q},A}^{(\alpha)}(t) = \int_0^\pi dk \min[|v_+(k) - v_-(k)|t, |A|] s_\alpha[n_{++}(k)], \quad (46)
$$

where $n_{++}(k)$ is the conserved (for $U = 0$) diagonal occupation number of $+$ particles [cf. (19)], the group velocities are given by

$$
v_\pm(k) \equiv \partial_k \epsilon_\pm(k) = \frac{\mp(1 - \delta^2)\sin(2k)}{\sqrt{\delta^2 + (1 - \delta^2)\cos^2(k)}} \\
+ 4J_2 \sin(2k), \quad (47)
$$

and we introduced

$$
s_\alpha[x] = \frac{x^\alpha + (1 - x)^\alpha}{\pi(1 - \alpha)}. \quad (48)
$$

Note that since

$$
n_{++}(k) + n_{--}(k) = 1, \quad (49)
$$

we have

$$
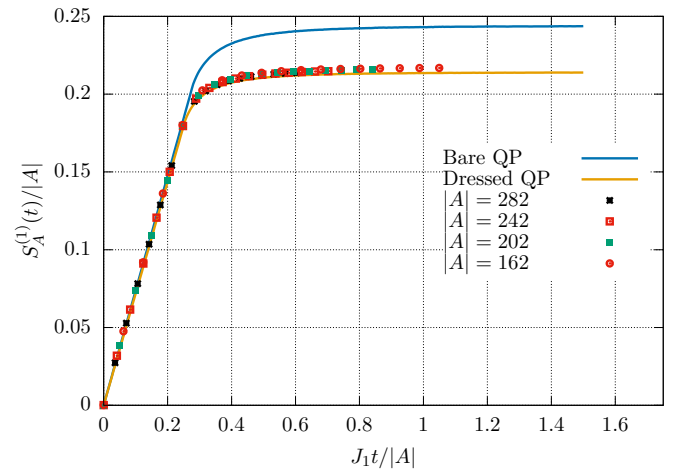s_\alpha[n_{++}(k)] = s_\alpha[n_{--}(k)], \quad (50)
$$

FIG. 5. Comparison between the solution of the first-order EOM (21) and the prediction of the quasiparticle picture for the rescaled entanglement entropy $S_A^{(1)}$ (von Neumann) after a quench (12) with parameters $J_{20} = 0$, $\delta_0 = 0.8$, $U_0 = 0$, $J_2 = 0$, $\delta = 0.1$, $U = 0.4$. The blue solid line is the prediction of bare quasiparticles while the orange solid line is the one of dressed quasiparticles. Points are the (rescaled) von Neumann entropies for $|A| = 162, 202, 242, 282$ obtained through Eq. (21).

and the prediction is symmetric in $+$ and $-$. Finally, since (46) only depends on the difference of $v_-(k)$ and $v_+(k)$, it is independent of J_2.

The question that we want to address here is whether a similar quasiparticle prediction can be devised for $0 < U \ll 1$. In our simple framework, everything is fully specified by $n_{\mu\nu}(k, t)$, therefore to understand whether a quasiparticle picture can work we need to look at how these quantities depend on time. Inspecting the perturbative solution (22) of the first-order EOM (21) we see that at large enough times it has the same form as the free one [cf. (18)] with the replacements

$$
\epsilon_\eta(k) \mapsto \epsilon_\eta^{\mathrm{dr}}(k), \quad n_{\mu\nu}(k) \mapsto n_{\mu\nu}^{\mathrm{dGGE}}(k), \quad (51)
$$

where $\epsilon_\eta^{\mathrm{dr}}(k)$ and $n_{\mu\nu}^{\mathrm{dGGE}}(k)$ are defined, respectively, in Eqs. (23) and (26) and we neglected $O(U^2)$ corrections. This means that for $0 \leqslant t \lesssim U^{-1}$, i.e., in the time regime where the first-order EOM give a good description of the results, we can define a quasiparticle picture by replacing $v_\pm(k)$ and $n_{\pm\pm}(k)$ with their dressed counterparts obtained from Eqs. (23) and (26). Namely,

$$
S_{\mathrm{dq},A}^{(\alpha)}(t) = \int_0^\pi dk \min[|v_+^{\mathrm{dr}}(k) - v_-^{\mathrm{dr}}(k)|t, |A|] s_\alpha[n_{++}^{\mathrm{dr}}(k)], \quad (52)
$$

with

$$
v_\eta^{\mathrm{dr}}(k) = \partial_k \epsilon_\eta^{\mathrm{dr}}(k), \quad n_{\mu\mu}^{\mathrm{dr}}(k) = n_{\mu\nu}^{\mathrm{dGGE}}(k). \quad (53)
$$

A comparison between bare and dressed quasiparticle predictions and the solution of the first-order EOM (21) is reported in Fig. 5. Note that in this case $n_{+-}^{\mathrm{dGGE}}(k) \neq 0$ and one would need to "diagonalize" the quasiparticle occupations as in Ref. [38]. This effect, however, gives a subleading correction in U and since we are working at $O(U)$ we can neglect it. Finally, we remark that a quasiparticle picture valid for times
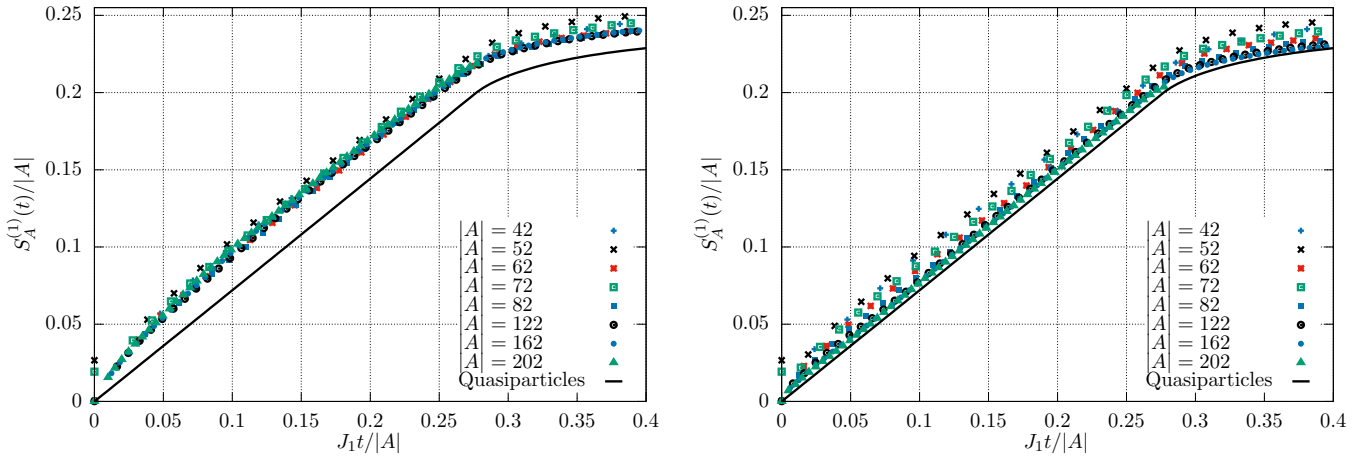
FIG. 6. Comparison between the scaling of the solutions of the second-order EOM (27) (left) and that of the first-order EOM (21) (right) where the black line is the "scattering quasiparticle" prediction of Eq. (56). The parameters of the quench are fixed to $J_{20} = 0$, $\delta_0 = 0.8$, $U_0 = 0$, $J_2 = 0.5$, $\delta = 0.1$, $U = 0.1$. The collapse of the first-order data is attained for $\ell_{\min} \approx 200$, while $\bar{v}U^{-2} \approx 100$.

$t \sim U^{-1}$ can be devised also when the system displays prerelaxation (see Ref. [90]). Namely, when, due to some special symmetries of the unperturbed Hamiltonian, the deformed GGE becomes (slowly) time dependent for $0 \leqslant t \lesssim U^{-1}$ [84].

For $t \gg U^{-1}$ the integrability breaking begins to dominate and, accordingly, the quasiparticles start to scatter inelastically approaching the equilibrium state. Consequently, the occupation numbers $n_{\pm\pm}(k)$ evolve from their deformed GGE values $n_{\pm\pm}^{\mathrm{dGGE}}(k)$ to their thermal values. In this situation it is natural to distinguish two different regimes for the behavior of the entanglement of the subsystem A,

$$\text{(i) } |A| \ll \bar{v}U^{-2} \quad \text{and} \quad \text{(ii) } |A| \gg \bar{v}U^{-2}, \quad (54)$$

where $\bar{v}$ is the minimal velocity of the quasiparticles giving a relevant contribution to the entanglement. In other words, $\bar{v}$ is the maximal v such that $S_{q,A}^{(\alpha)}(|A|/v)$ essentially equals its saturation value. For the quenches considered here $\bar{v} \approx 1$ (for example, $\bar{v} \approx 1.2$ in the case of Fig. 5).

In the case (i) the effects of the interactions are negligible for all the time needed by A to relax to the deformed GGE. Accordingly, we expect the slopes of the entanglement entropies to be described by the dressed quasiparticle prediction (52). The integrability breaking effects become dominant when the subsystem has already relaxed to the deformed GGE and cause a slow drift toward the thermal state. At the leading order in U, such a drift is described by the QBE (34). Since during the drift the state is quasistationary, we expect that for $t \sim U^{-2}$ the entropies can be computed as

$$S_A^{(\alpha)}(t \sim U^{-2}) = |A| \int_0^\pi \frac{dk}{2} \big(s_\alpha[n_{++}(k, U^2 t)]$$
$$+ s_\alpha[n_{--}(k, U^2 t)] \big) + O(U), \quad (55)$$

where $\{n_{\pm\pm}(q, \tau)\}$ are obtained by solving the Boltzmann equation (34). Equation (55) is just the thermodynamic Rényi entropy of a free stationary state with occupation numbers $\{n_{\pm\pm}(k, \tau)\}$. Noting that $\{n_{\pm\pm}(q, \tau)\}$ are almost constant for times $t < |A|/v$ we can combine (55) with (52). In this way, we obtain the following quasiparticle prediction valid for all

times:

$$S_{\mathrm{Bq},A}^{(\alpha)}(t) = \int_0^\pi \frac{dk}{2} \min(|v_+^{\mathrm{dr}}(k, U^2 t) - v_-^{\mathrm{dr}}(k, U^2 t)|t, |A|)$$
$$\times (s_\alpha[n_{++}^{\mathrm{dr}}(k, U^2 t)] + s_\alpha[n_{--}^{\mathrm{dr}}(k, \tau)]). \quad (56)$$

Here $v_\pm^{\mathrm{dr}}(k, \tau)$ and $n_{++}^{\mathrm{dr}}(k, \tau)$ are obtained by replacing $n_\pm(k)$ with $n_\pm(k, \tau)$ in (53) [cf. (23) and (26)]. In this way (56) is accurate up to $O(U)$ for $t \sim U^{-1}$ [for small enough U the dressing effects become negligible and one can safely use $v_\pm(k)$ and $n_{++}(k, \tau)$ in Eq. (56)]. Note that in this regime (56) agrees with (52) because

$$s_\alpha[n_{++}^{\mathrm{dr}}(k, 0)] = \frac{s_\alpha[n_{++}^{\mathrm{dr}}(k, 0)] + s_\alpha[n_{--}^{\mathrm{dr}}(k, 0)]}{2}. \quad (57)$$

In the case (ii) the effects of the interactions become significant much before the quasirelaxation of A to the deformed GGE and hence we do not expect the quasiparticle picture (even the dressed one) to correctly describe the slope of the entanglement entropies. Indeed, the latter completely neglects all other mechanisms for spreading and production of entanglement that are active in the nonintegrable regime. Nevertheless, for large enough times we still expect the system to relax to a quasistationary state described by the Boltzmann equation and (55) to apply.

The above considerations imply that the verification of (56) by means of the equations of motion (27) requires some care. One needs to consider $|A| > \ell_{\min}$ such that the quasiparticle picture can hold, but, at the same time, always keep $|A| \ll \bar{v}U^{-2}$. An intuitive way to estimate $\ell_{\min}$ is to look at the collapse of $S_A^{(\alpha)}(t)/|A|$ as a function of $t/|A|$. However, it turns out that, at fixed values of the parameters, the values of $|A|$ at which we observe the collapse depend on the specific EOM used: the solution of the second-order EOM (27) attains its scaling form much before (i.e., form for much smaller $|A|$) that of the first-order EOM (21) (see, e.g., Fig. 6). Since the first-order equations are asymptotically described by the quasiparticle picture, we conjecture that the minimal length is set by the collapse of the latter.
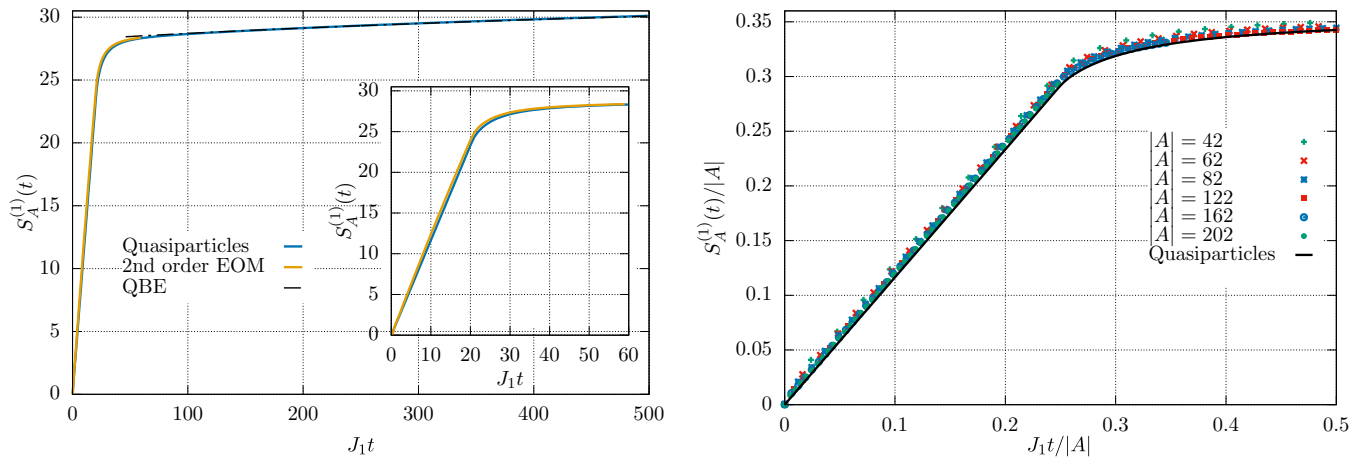
FIG. 7. Right: Comparison between the solution of the second-order EOM (27) (orange), the quantum Boltzmann equation (34) (dashed-dotted line), and the prediction of the "scattering quasiparticle" picture (56) (blue). The pictures report the behavior of the entanglement entropy $S_A^{(1)}$ (von Neumann) of a subsystem of size $|A| = 120$ after a quench (12) with parameters $J_{20} = 0, \delta_0 = 0.8, U_0 = 0, J_2 = 0.5, \delta = 0, U = 0.05$. Left: Collapse of the rescaled von Neumann entropy computed via first-order equations for different subsystems $|A| = 42, 62, 82, 102$ (points) compared with (56) (blue). The collapse in the first-order data is attained for $\ell_{\min} \approx 100$, while $\bar{v}U^{-2} \approx 400$.

Identifying in this way the regime (ii) we find that (56) shows a satisfactory agreement with the results of EOM and QBE (for a representative example see Fig. 7). As expected, however, for $|A| > \bar{v}U^{-2}$ Eq. (56) describes quantitatively only the late-time regime ($t \sim U^{-2}$) (see Fig 8). Interestingly, the behavior reported in Fig. 8 appears to be general: in the initial and intermediate time regimes the quasiparticle picture gives a lower bound for the entanglement growth. This can be understood by imagining that together with the entanglement growth due to the spreading quasiparticles there is a further increase of the entanglement due to integrability-breaking effects.
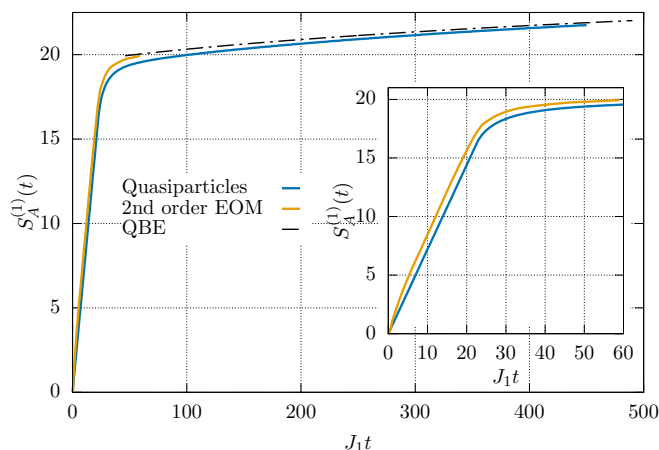
We conclude this section by recalling that the quasiparticle approach we developed is expected to work exactly in the same manner every time that the unperturbed model is described by free particles (and can be also used for more complicated entanglement measures, such as the negativity [137]). Instead, when the unperturbed model is an interacting integrable one, it is only known how to adapt the quasiparticle picture to the time evolution of the von Neumann entropy [40,41], while for Rényi entropies there are still open issues (see, e.g., Refs. [45,138–140]).

V. CONCLUSIONS

In this paper we studied the spreading and generation of entanglement in a weakly interacting system of lattice fermions using equations-of-motion techniques [88,88,89,109–117]. We found that for small enough interactions, parametrized by their strength U, the entanglement entropies show the typical prethermalization behavior [75]: they first approach a quasistationary plateau described by a deformed GGE and then, on a separate timescale $\tau_{th} \sim U^{-2}$, they start relaxing toward their thermal value. This behavior has been interpreted by means of a modified quasiparticle picture where the contribution of each pair to the entanglement, normally time independent, depends on $U^2 t$ and is obtained by solving a quantum Boltzmann equation. This modified quasiparticle picture predicts the correct quantitative behavior of the entanglement entropies of the subsystem A whenever τ_A, the timescale over which A relaxes to the deformed GGE, is much smaller than τ_{th}, the timescale associated with integrability breaking. In the opposite case, it describes quantitatively only the late-time regime while it underestimates the slope of the entanglement entropies.

There are two immediate future directions for the research presented in our work. First, it would be interesting to generalize our findings to the case of weak perturbations to strongly interacting integrable systems, combining our modified quasiparticle picture with the recent results [97–99] on the quantum

FIG. 8. Comparison between the solution of the second-order EOM (27) (orange), the quantum Boltzmann equation (34) (dashed-dotted line), and the prediction of the "scattering quasiparticle" picture (56) (blue). The pictures report the behavior of the entanglement entropy $S_A^{(1)}$ (von Neumann) of a subsystem of size $|A| = 120$ after a quench (12) with parameters $J_{20} = 0, \delta_0 = 0.8, U_0 = 0, J_2 = 0.5, \delta = 0.1, U = 0.1$. The collapse in the first-order data is attained for $\ell_{\min} \approx 200$, while $\bar{v}U^{-2} \approx 100$.

Boltzmann equation for interacting integrable models. Second, it would be interesting to search for a simple description of the integrability-breaking correction that we observed in the slope of the entanglement entropies for $\tau_A > \tau_{\text{th}}$. Note that similar integrability-breaking effects are also visible in equal-time two-point functions for large enough separation of the two points.

[1] A. Polkovnikov, K. Sengupta, A. Silva, and M. Vengalattore, Colloquium: Nonequilibrium dynamics of closed interacting quantum systems, Rev. Mod. Phys. **83**, 863 (2011).

[2] C. Gogolin and J. Eisert, Equilibration, thermalisation, and the emergence of statistical mechanics in closed quantum systems, Rep. Prog. Phys. **79**, 056001 (2016).

[3] L. D'Alessio, Y. Kafri, A. Polkovnikov, and M. Rigol, From quantum chaos and eigenstate thermalization to statistical mechanics and thermodynamics, Adv. Phys. **65**, 239 (2016).

[4] P. Calabrese, F. Essler, and G. Mussardo, Introduction to 'Quantum integrability in out of equilibrium systems' J. Stat. Mech. (2016) 064001.

[5] P. Calabrese, Entanglement and thermodynamics in non-equilibrium isolated quantum systems, Physica A (Amsterdam) **504**, 31 (2018).

[6] J. M. Deutsch, H. Li, and A. Sharma, Microscopic origin of thermodynamic entropy in isolated systems, Phys. Rev. E **87**, 042135 (2013).

[7] W. Beugeling, A. Andreanov, and M. Haque, Global characteristics of all eigenstates of local many-body Hamiltonians: participation ratio and entanglement entropy, J. Stat. Mech. (2015) P02002.

[8] V. Gurarie, Global large time dynamics and the generalized Gibbs ensemble, J. Stat. Mech. (2013) P02014.

[9] L. F. Santos, A. Polkovnikov, and M. Rigol, Entropy of Isolated Quantum Systems after a Quench, Phys. Rev. Lett. **107**, 040601 (2011).

[10] M. Collura, M. Kormos, and P. Calabrese, Stationary entropies following an interaction quench in 1*D* Bose gas, J. Stat. Mech. (2014) P01009.

[11] A. M. Kaufman, M. E. Tai, A. Lukin, M. Rispoli, R. Schittko, P. M. Preiss, and M. Greiner, Quantum thermalisation through entanglement in an isolated many-body system, Science **353**, 794 (2016).

[12] C. T. Asplund, A. Bernamonti, F. Galli, and T. Hartman, Entanglement scrambling in 2D conformal field theory, J. High Energy Phys. 09 (2015) 110.

[13] V. Hubeny, M. Rangamani, and T. Takayanagi, A covariant holographic entanglement entropy proposal, J. High Energy Phys. 07 (2007) 062.

[14] J. Abajo-Arrastia, J. Aparício, and E. López, Holographic evolution of entanglement entropy, J. High Energy Phys. 11 (2010) 149.

[15] T. Hartman and J. Maldacena, Time evolution of entanglement entropy from black hole interiors, J. High Energy Phys. 05 (2013) 014.

[16] H. Liu and S. J. Suh, Entanglement Tsunami: Universal Scaling in Holographic Thermalization, Phys. Rev. Lett. **112**, 011601 (2014).

[17] S. Leichenauer and M. Moosa, Entanglement tsunami in (1+1)-dimensions, Phys. Rev. D **92**, 126004 (2015).

[18] H. Casini, H. Liu, and M. Mezei, Spread of entanglement and causality, J. High Energy Phys. 07 (2016) 077.

[19] P. Hayden and J. Preskill, Black holes as mirrors: Quantum information in random subsystems, J. High Energy Phys. 09 (2007) 120.

[20] Y. Sekino and L. Susskind, Fast scramblers, J. High Energy Phys. 10 (2008) 065.

[21] V. Alba and P. Calabrese, Quantum information scrambling after a quantum quench, Phys. Rev. B **100**, 115150 (2019).

[22] R. Modak, V. Alba, and P. Calabrese, Entanglement revivals as a probe of scrambling in finite quantum systems, J. Stat. Mech. (2020) 083110.

[23] N. Schuch, M. M. Wolf, F. Verstraete, and J. I. Cirac, Entropy Scaling and Simulability by Matrix Product States, Phys. Rev. Lett. **100**, 030504 (2008).

[24] N. Schuch, M. M. Wolf, K. G. H. Vollbrecht, and J. I. Cirac, On entropy growth and the hardness of simulating time evolution, New J. Phys. **10**, 033032 (2008).

[25] A. Perales and G. Vidal, Entanglement growth and simulation efficiency in one-dimensional quantum lattice systems, Phys. Rev. A **78**, 042337 (2008).

[26] P. Hauke, F. M. Cucchietti, L. Tagliacozzo, I. Deutsch, and M. Lewenstein, Can one trust quantum simulators? Prog. Phys. **75**, 082401 (2012).

[27] J. Dubail, Entanglement scaling of operators: A conformal field theory approach, with a glimpse of simulability of long-time dynamics in 1+1d, J. Phys. A: Math. Theor. **50**, 234001 (2017).

[28] P. Calabrese and J. Cardy, Evolution of entanglement entropy in one-dimensional systems, J. Stat. Mech. (2005) P04010.

[29] M. Fagotti and P. Calabrese, Evolution of entanglement entropy following a quantum quench: Analytic results for the XY chain in a transverse magnetic field, Phys. Rev. A **78**, 010306(R) (2008).

[30] V. Eisler and I. Peschel, Entanglement in a periodic quench, Ann. Phys. (Berlin) **17**, 410 (2008).

[31] M. G. Nezhadhaghighi and M. A. Rajabpour, Entanglement dynamics in short- and long-range harmonic oscillators, Phys. Rev. B **90**, 205438 (2014).

[32] L. Bucciantini, M. Kormos, and P. Calabrese, Quantum quenches from excited states in the Ising chain, J. Phys. A: Math. Theor. **47**, 175002 (2014).

[33] E. Bianchi, L. Hackl, and N. Yokomizo, Linear growth of the entanglement entropy and the Kolmogorov-Sinai rate, J. High Energy Phys. 03 (2018) 25.

[34] L. Hackl, E. Bianchi, R. Modak, and M. Rigol, Entanglement production in bosonic systems: Linear and logarithmic growth, Phys. Rev. A **97**, 032321 (2018).

[35] A. S. Buyskikh, M. Fagotti, J. Schachenmayer, F. Essler, and A. J. Daley, Entanglement growth and correlation spreading with variable-range interactions in spin and fermionic tunneling models, Phys. Rev. A **93**, 053620 (2016).

[36] J. S. Cotler, M. P. Hertzberg, M. Mezei, and M. T. Mueller, Entanglement growth after a global quench in free scalar field theory, J. High Energy Phys. 11 (2016) 166.

[37] B. Bertini, E. Tartaglia, and P. Calabrese, Entanglement and diagonal entropies after a quench with no pair structure, J. Stat. Mech. (2018) 063104.

[38] A. Bastianello and P. Calabrese, Spreading of entanglement and correlations after a quench with intertwined quasiparticles, SciPost Phys. **5**, 033 (2018).

[39] B. Bertini, M. Fagotti, L. Piroli, and P. Calabrese, Entanglement evolution and generalised hydrodynamics: noninteracting systems, J. Phys. A: Math. Theor. **51**, 39LT01 (2018).

[40] V. Alba and P. Calabrese, Entanglement and thermodynamics after a quantum quench in integrable systems, Proc. Natl. Acad. Sci. USA **114**, 7947 (2017).

[41] V. Alba and P. Calabrese, Entanglement dynamics after quantum quenches in generic integrable systems, SciPost Phys. **4**, 017 (2018).

[42] M. Mestyan, B. Bertini, L. Piroli, and P. Calabrese, Exact solution for the quench dynamics of a nested integrable system, J. Stat. Mech. (2017) 083103.

[43] C. P. Moca, M. Kormos, and G. Zarand, Hybrid Semiclassical Theory of Quantum Quenches in One-Dimensional Systems, Phys. Rev. Lett. **119**, 100603 (2017).

[44] V. Alba, Entanglement and quantum transport in integrable systems, Phys. Rev. B **97**, 245135 (2018).

[45] V. Alba, B. Bertini, and M. Fagotti, Entanglement evolution and generalised hydrodynamics: Interacting integrable systems, SciPost Phys. **7**, 005 (2019).

[46] A. M. Läuchli and C. Kollath, Spreading of correlations and entanglement after a quench in the one-dimensional Bose-Hubbard model, J. Stat. Mech. (2008) P05018.

[47] H. Kim and D. A. Huse, Ballistic Spreading of Entanglement in a Diffusive Nonintegrable System, Phys. Rev. Lett. **111**, 127205 (2013).

[48] M. Collura, M. Kormos, and G. Takacs, Dynamical manifestation of the Gibbs paradox after a quantum quench, Phys. Rev. A **98**, 053610 (2018).

[49] I. Frerot, P. Naldesi, and T. Roscilde, Multispeed Prethermalization in Quantum Spin Models with Power-Law Decaying Interactions, Phys. Rev. Lett. **120**, 050401 (2018).

[50] R. Pal and A. Lakshminarayan, Entangling power of time-evolution operators in integrable and nonintegrable many-body systems, Phys. Rev. B **98**, 174304 (2018).

[51] B. Bertini, P. Kos, and T. Prosen, Entanglement Spreading in a Minimal Model of Maximal Many-Body Quantum Chaos, Phys. Rev. X **9**, 021033 (2019).

[52] S. Gopalakrishnan and A. Lamacraft, Unitary circuits of finite depth and infinite width from quantum channels, Phys. Rev. B **100**, 064309 (2019).

[53] T. Brydges, A. Elben, P. Jurcevic, B. Vermersch, C. Maier, B. P. Lanyon, P. Zoller, R. Blatt, and C. F. Roos, Probing entanglement entropy via randomized measurements, Science **364**, 260 (2019).

[54] L. Piroli, B. Bertini, J. I. Cirac, and T. Prosen, Exact dynamics in dual-unitary quantum circuits, Phys. Rev. B **101**, 094304 (2020).

[55] F. M. Surace, P. P. Mazza, G. Giudici, A. Lerose, A. Gambassi, and M. Dalmonte, Lattice Gauge Theories and String Dynamics in Rydberg Atom Quantum Simulators, Phys. Rev. X **10**, 021041 (2020).

[56] G. De Chiara, S. Montangero, P. Calabrese, and R. Fazio, Entanglement entropy dynamics of Heisenberg chains, J. Stat. Mech. (2006) P03001.

[57] M. Znidarič, T. Prosen, and P. Prelovšek, Many-body localization in the Heisenberg XXZ magnet in a random field, Phys. Rev. B **77**, 064426 (2008).

[58] J. H. Bardarson, F. Pollmann, and J. E. Moore, Unbounded Growth of Entanglement in Models of Many-Body Localization, Phys. Rev. Lett. **109**, 017202 (2012).

[59] F. Iglói, G. Roósz, and Y.-C. Lin, Non-equilibrium quench dynamics in quantum quasicrystals, New J. Phys. **15**, 023036 (2013).

[60] G. Roósz, U. Divakaran, H. Rieger, and F. Iglói, Nonequilibrium quantum relaxation across a localization-delocalization transition, Phys. Rev. B **90**, 184202 (2014).

[61] R. Vosk and E. Altman, Dynamical Quantum Phase Transitions in Random Spin Chains, Phys. Rev. Lett. **112**, 217204 (2014).

[62] R. Nandkishore and D. A. Huse, Many-body localization and thermalization in quantum statistical mechanics, Annu. Rev. Condens. Matter Phys. **6**, 15 (2015).

[63] F. Igloi, Z. Szatmari, and Y.-C. Lin, Entanglement entropy dynamics of disordered quantum spin chains, Phys. Rev. B **85**, 094417 (2012).

[64] A. Nahum, J. Ruhman, and D. A. Huse, Dynamics of entanglement and transport in one-dimensional systems with quenched randomness Phys. Rev. B **98**, 035118 (2018).

[65] M. Kormos, M. Collura, G. Takács, and P. Calabrese, Real-time confinement following a quantum quench to a nonintegrable model, Nat. Phys. **13**, 246 (2017).

[66] A. J. A. James, R. M. Konik, and N. J. Robinson, Nonthermal States Arising from Confinement in One and Two Dimensions, Phys. Rev. Lett. **122**, 130603 (2019).

[67] O. A. Castro-Alvaredo, M. Lencses, I. M. Szecsenyi, and J. Viti, Entanglement Oscillations Near a Quantum Critical Point, Phys. Rev. Lett. **124**, 230601 (2020).

[68] A. Lerose, F. M. Surace, P. P. Mazza, G. Perfetto, M. Collura, and A. Gambassi, Quasilocalized dynamics from confinement of quantum excitations, Phys. Rev. B **102**, 041118(R) (2020).

[69] T. Chanda, J. Zakrzewski, M. Lewenstein, and L. Tagliacozzo, Confinement and Lack of Thermalization after Quenches in the Bosonic Schwinger Model, Phys. Rev. Lett. **124**, 180602 (2020).

[70] C. J. Turner, A. A. Michailidis, D. A. Abanin, M. Serbyn, and Z. Papic, Quantum many-body scars, Nat. Phys. **14**, 745 (2018).

[71] S. Choi, C. J. Turner, H. Pichler, W. W. Ho, A. A. Michailidis, Z. Papic, M. Serbyn, M. D. Lukin, and D. A. Abanin, Emergent SU(2) Dynamics and Perfect Quantum Many-Body Scars, Phys. Rev. Lett. **122**, 220603 (2019).

[72] A. Nahum, J. Ruhman, S. Vijay, and J. Haah, Quantum Entanglement Growth under Random Unitary Dynamics, Phys. Rev. X **7**, 031016 (2017).

[73] A. Nahum, S. Vijay, and J. Haah, Operator Spreading in Random Unitary Circuits, Phys. Rev. X **8**, 021014 (2018).

[74] T. Zhou and A. Nahum, The entanglement membrane in chaotic many-body systems, arXiv:1912.12311.

[75] M. Moeckel and S. Kehrein, Interaction Quench in the Hubbard Model, Phys. Rev. Lett. **100**, 175702 (2008); Real-time evolution for weak interaction quenches in quantum systems, Ann. Phys. **324**, 2146 (2009).

[76] A. Rosch, D. Rasch, B. Binz, and M. Vojta, Metastable Superfluidity of Repulsive Fermionic Atoms in Optical Lattices, Phys. Rev. Lett. **101**, 265301 (2008).

[77] M. Kollar, F. A. Wolf, and M. Eckstein, Generalized Gibbs ensemble prediction of prethermalization plateaus and their relation to nonthermal steady states in integrable systems, Phys. Rev. B **84**, 054304 (2011).

[78] M. van den Worm, B. C. Sawyer, J. J. Bollinger, and M. Kastner, Relaxation timescales and decay of correlations in a long-range interacting quantum simulator, New J. Phys. **15**, 083007 (2013).

[79] M. Marcuzzi, J. Marino, A. Gambassi, and A. Silva, Prethermalization in a Nonintegrable Quantum Spin Chain after a Quench, Phys. Rev. Lett. **111**, 197203 (2013).

[80] F. H. L. Essler, S. Kehrein, S. R. Manmana, and N. J. Robinson, Quench dynamics in a model with tuneable integrability breaking, Phys. Rev. B **89**, 165104 (2014).

[81] N. Nessi, A. Iucci and M. A. Cazalilla, Quantum Quench and Prethermalization Dynamics in a Two-Dimensional Fermi Gas with Long-Range Interactions, Phys. Rev. Lett. **113**, 210402 (2014).

[82] M. Fagotti, On conservation laws, relaxation and prerelaxation after a quantum quench, J. Stat. Mech. (2014) P03016.

[83] G. P. Brandino, J.-S. Caux, and R. M. Konik, Glimmers of a Quantum KAM Theorem: Insights from Quantum Quenches in One-Dimensional Bose Gases, Phys. Rev. X **5**, 041043 (2015).

[84] B. Bertini and M. Fagotti, Pre-relaxation in weakly interacting models, J. Stat. Mech. (2015) P07012.

[85] A. Chiocchetta, M. Tavora, A. Gambassi, and A. Mitra, Short-time universal scaling in an isolated quantum system after a quench, Phys. Rev. B **91**, 220302(R) (2015); **92**, 219901(E) (2015).

[86] M. Babadi, E. Demler, and M. Knap, Far-from-Equilibrium Field Theory of Many-Body Quantum Spin Systems: Prethermalization and Relaxation of Spin Spiral States in Three Dimensions, Phys. Rev. X **5**, 041005 (2015).

[87] P. Smacchia, M. Knap, E. Demler, and A. Silva, Exploring dynamical phase transitions and prethermalization with quantum noise of excitations, Phys. Rev. B **91**, 205136 (2015).

[88] B. Bertini, F. H. L. Essler, S. Groha, and N. J. Robinson, Prethermalization and Thermalization in Models with Weak Integrability Breaking, Phys. Rev. Lett. **115**, 180601 (2015).

[89] B. Bertini, F. H. L. Essler, S. Groha, and N. J. Robinson, Thermalization and light cones in a model with weak integrability breaking, Phys. Rev. B **94**, 245117 (2016).

[90] M. Fagotti and M. Collura, Universal prethermalization dynamics of entanglement entropies after a global quench, arXiv:1507.02678.

[91] G. Menegoz and A. Silva, Prethermalization of weakly interacting bosons after a sudden interaction quench, J. Stat. Mech. (2015) P05035.

[92] E. Kaminishi, T. Mori, T. Ikeda, N. Tatsuhiko, and M. Ueda, Entanglement pre-thermalization in a one-dimensional Bose gas, Nat. Phys. **11**, 1050 (2015).

[93] G. Delfino, Quantum quenches with integrable pre-quench dynamics, J. Phys. A: Math. Theor. **47**, 402001 (2014).

[94] G. Delfino and J. Viti, On the theory of quantum quenches in near-critical systems, J. Phys. A: Math. Theor. **50**, 084004 (2017).

[95] V. Alba and M. Fagotti, Prethermalization at Low Temperature: The Scent of Long-Range Order, Phys. Rev. Lett. **119**, 010601 (2017).

[96] K. Mallayya, M. Rigol, and W. De Roeck, Prethermalization and Thermalization in Isolated Quantum Systems, Phys. Rev. X **9**, 021027 (2019).

[97] A. J. Friedman, S. Gopalakrishnan, and R. Vasseur, Diffusive hydrodynamics from integrability breaking, Phys. Rev. B **101**, 180302 (2020).

[98] J. Durnin, M. J. Bhaseen, and B. Doyon, Non-equilibrium dynamics and weakly broken integrability, arXiv:2004.11030.

[99] J. Lopez-Piqueres, B. Ware, S. Gopalakrishnan, and R. Vasseur, Hydrodynamics of non-integrable systems from relaxation-time approximation, arXiv:2005.13546.

[100] P. Ruggiero, L. Foini, and T. Giamarchi, Thermalization, prethermalization and impact of the temperature in the quench dynamics of two unequal Luttinger liquids, arXiv:2006.16088.

[101] M. Gring, M. Kuhnert, T. Langen, T. Kitagawa, B. Rauer, M. Schreitl, I. Mazets, D. A. Smith, E. Demler, and J. Schmiedmayer, Relaxation Dynamics and Pre-thermalisation in an Isolated Quantum System, Science **337**, 1318 (2012).

[102] T. Langen, T. Gasenzer, and J. Schmiedmayer, Prethermalization and universal dynamics in near-integrable quantum systems, J. Stat. Mech. (2016) 064009.

[103] Y. Tang, W. Kao, K.-Y. Li, S. Seo, K. Mallayya, M. Rigol, S. Gopalakrishnan, and B. L. Lev, Thermalization near Integrability in a Dipolar Quantum Newton's Cradle, Phys. Rev. X **8**, 021030 (2018).

[104] I. Bloch, J. Dalibard, and W. Zwerger, Many-body physics with ultracold gases, Rev. Mod. Phys. **80**, 885 (2008).

[105] T. Kinoshita, T. Wenger, and D. S. Weiss, A quantum Newton's cradle, Nature (London) **440**, 900 (2006).

[106] M. Schemmer, I. Bouchoule, B. Doyon, and J. Dubail, Generalized HydroDynamics on an Atom Chip, Phys. Rev. Lett. **122**, 090601 (2019).

[107] T. Langen, S. Erne, R. Geiger, B. Rauer, T. Schweigier, M. Kuhnert, W. Rohringer, I. E. Mazets, T. Gasenzer, and J. Schmiedmayer, Experimental observation of a generalized Gibbs ensemble, Science **348**, 207 (2015).

[108] B. Bertini, P. Kos, and T. Prosen, Exact Correlation Functions for Dual-Unitary Lattice Models in $1+1$ Dimensions, Phys. Rev. Lett. **123**, 210601 (2019).

[109] M. Stark and M. Kollar, Kinetic description of thermalization dynamics in weakly interacting quantum systems, arXiv:1308.1610.

[110] N. Nessi and A. Iucci, Glass-like behavior in a system of one dimensional fermions after a quantum quench, arXiv:1503.02507.

[111] A. Iucci and N. Nessi, Equations of motion for the out-of-equilibrium dynamics of isolated quantum systems from the projection operator technique, J. Phys.: Conf. Ser. **568**, 012013 (2014).

[112] L. Erdős, M. Salmhofer, and H.-T. Yau, On the quantum boltzmann equation, J. Stat. Phys. **116**, 367 (2004).

[113] J. Lukkarinen and H. Spohn, Not to normal order–notes on the kinetic limit for weakly interacting quantum fluids, J. Stat. Phys. **134**, 1133 (2009).

[114] M. L. R. Fürst, C. B. Mendl, and H. Spohn, Matrix-valued Boltzmann equation for the Hubbard chain, Phys. Rev. E **86**, 031122 (2012).

[115] M. L. R. Fürst, C. B. Mendl, and H. Spohn, Matrix-valued Boltzmann equation for the nonintegrable Hubbard chain, Phys. Rev. E **88**, 012108 (2013).

[116] L. P. Kadanoff and G. A. Baym, *Quantum Statistical Mechanics* (Benjamin, New York, 1962).

[117] M. Bonitz, *Quantum Kinetic Theory* (Teubner, Stuttgart, 1998).

[118] R. Orbach, Linear antiferromagnetic chain with anisotropic coupling, Phys. Rev. **112**, 309 (1958).

[119] F. H. L. Essler and R. M. Konik, in *From Fields to Strings: Circumnavigating Theoretical Physics*, edited by M. Shifman, A. Vainshtein, and J. Wheater (World Scientific, Singapore, 2005); Applications of Massive Integrable Quantum Field Theories to Problems in Condensed Matter Physics, arXiv:cond-mat/0412421.

[120] F. H. L. Essler and M. Fagotti, Quench dynamics and relaxation in isolated integrable quantum spin chains, J. Stat. Mech. (2016) 064002.

[121] S. Sotiriadis and P. Calabrese, Validity of the GGE for quantum quenches from interacting to noninteracting models, J. Stat. Mech. (2014) P07024.

[122] K. Sengupta, S. Powell, S. Sachdev, Quench dynamics across quantum critical points, Phys. Rev. A **69**, 053616 (2004).

[123] P. Calabrese, F. H. L. Essler, and M. Fagotti, Quantum Quench in the Transverse Field Ising chain I: Time evolution of order parameter correlators, J. Stat. Mech. (2012) P07016.

[124] S. Sotiriadis, G. Takacs, and G. Mussardo, Boundary state in an integrable quantum field theory out of equilibrium, Phys. Lett. B **734**, 52 (2014).

[125] B. Bertini, Non-equilibrium dynamics of interacting many-body quantum systems in one dimension, Ph.D. thesis, University of Oxford, 2015.

[126] F. Wegner, Flow-equations for Hamiltonians, Ann. Phys. (Berlin) **506**, 77 (1994).

[127] C. Knetter and G. S. Uhrig, Perturbation theory by flow equations: dimerized and frustrated S = 1/2 chain, Eur. Phys. J. B **13**, 209 (2000).

[128] C. P. Heidbrink and G. S. Uhrig, Renormalization by continuous unitary transformations: one-dimensional spinless fermions, Eur. Phys. J. B **30**, 443 (2002).

[129] S. Kehrein, *The Flow-equation Approach to Many-particle Systems* (Springer, Berlin, 2007).

[130] B. K. Shivamoggi, *Perturbation Methods for Differential Equations* (Birkhäuser, Boston, 2003).

[131] J. Lux, J. Müller, A. Mitra, and A. Rosch, Hydrodynamic long-time tails after a quantum quench, Phys. Rev. A **89**, 053608 (2014).

[132] H. Kim, M. C. Bañuls, J. I. Cirac, M. B. Hastings, and D. A. Huse, Slowest local operators in quantum spin chains, Phys. Rev. E **92**, 012128 (2015).

[133] I. Peschel, Calculation of reduced density matrices from correlation functions, J. Phys. A: Math. Gen. **36**, L205 (2003).

[134] J. I. Latorre, E. Rico, and G. Vidal, Ground state entanglement in quantum spin chains, Quantum Inf. Comput. **4**, 048 (2004).

[135] I. Peschel and V. Eisler, Reduced density matrices and entanglement entropy in free lattice models, J. Phys. A: Math. Theor. **42**, 504003 (2009).

[136] F. R. A. Biebl and S. Kehrein, Thermalization rates in the one dimensional Hubbard model with next-to-nearest neighbor hopping, Phys. Rev. B **95**, 104304 (2017).

[137] V. Alba and P. Calabrese, Quantum information dynamics in multipartite integrable systems, Europhys. Lett. **126**, 60001 (2019).

[138] V. Alba and P. Calabrese, Quench action and Rényi entropies in integrable systems, Phys. Rev. B **96**, 115421 (2017).

[139] V. Alba and P. Calabrese, Rényi entropies after releasing the Néel state in the XXZ spin-chain, J. Stat. Mech. (2017) 113105.

[140] M. Mestyan, V. Alba, and P. Calabrese, Rényi entropies of generic thermodynamic macrostates in integrable systems, J. Stat. Mech. (2018) 083104.